The paper was published in the proceedings of the 7th International Conference on Earthquake Geotechnical Engineering and was edited by Francesco Silvestri, Nicola Moraci and Susanna Antonielli. The conference was held in Rome, Italy, 17 – 20 June 2019.

Earthquake Geotechnical Engineering for Protection and Development of Environment and Constructions – Silvestri & Moraci (Eds)

Effects of particle shape on the liquefaction resistance of sands

X. Wei
Department of Civil and Environmental Engineering, The University of Hong Kong, Hong Kong SAR
Department of Civil and Environmental Engineering, National University of Singapore, Singapore

J. Yang & Y.S. Zhuang
Department of Civil and Environmental Engineering, The University of Hong Kong, Hong Kong SAR

Y.G. Zhou & Y.M. Chen
MOE Key Laboratory of Soft Soils and Geoenvironmental Engineering, Institute of Geotechnical Engineering, Zhejiang University, Hangzhou, P.R. China

ABSTRACT: The cyclic behavior and liquefaction resistance of sands is a subject area of long-standing interest. Difficulties in estimating the liquefaction resistance of sands arise from the combined effects of various factors such as gradation, particle shape, fines content, plasticity, and so on, as well as from a lack of a proper framework for analysis. This paper presents a study that was aimed to investigate the cyclic behavior and liquefaction resistance of clean sands which share the same particle size distribution but different particle shapes. The particle shape was measured by using an imaging-based method. Undrained cyclic triaxial tests were conducted to evaluate the cyclic liquefaction resistance ratio. The test results showed that cyclic resistance decreased with increasing the overall regularity of particles when compared at the same void ratio. But characterization of the cyclic resistance of the sands using the traditional packing-density based method is difficult partly due to the complicated effect of confining pressure. One of the remarkable findings of this study is that the correlation between cyclic resistance and state parameter does not appear to be affected by particle shape, suggesting that the state parameter, defined with reference to the critical state line, is a suitable state variable to unify the liquefaction resistance for sands with different particle shapes. A critical-state-based framework proposed by Yang & Sze (2011a,b) was extended for liquefaction resistance evaluation taking into account the effects of particle shape.

1 INTRODUCTION

Soil liquefaction has long been a subject of interest since the Niigata and Alaska earthquakes of 1964. After decades of investigations, however, difficulties remain in liquefaction assessment, as a result of combined effects of many factors (e.g., soil properties, initial state of soil, and so on), as well as a lack of framework with theoretical background for analysis.

As a reflection of the formation history, the soil properties have significant influences on the mechanical behaviors of soil by affecting the packing patterns and interactions of the constituent particles. Among various soil properties, such as fines content, gradation, particle size, and mineralogy, the particle shape is relatively less investigated, which has been found to affect the mechanical behaviors of sands (e.g., Holubec & D'Appolonia 1973, Youd 1973, Hird & Hassona 1990) and has received increasing attentions in recent years (e.g., Cho et al. 2006, Rousé et al. 2008, Yang & Wei 2012, Yang & Luo, 2015). Arulmoli et al. (1985) proposed a correlation between cyclic resistance ratio and a composite electrical parameter which accounted for particle shape, porosity, and anisotropy. Kramer (1996) attributed the higher liquefaction susceptibility of soils with rounded particles to the easier densification of the soil, and related the frequently observed liquefaction in the fluvial and alluvial area to the frequently occurred particle rounding in the such environments. Partly because of difficulties in characterizing the particle shape, there lack systematic investigations into the effects of particle shape on liquefaction resistance of sand.

Unlike the gradational properties of soils (e.g., fines content and particle size), which can be confidently determined by routine methods (e.g., sieving test), the particle shape is not easy to be characterized quantitatively and is commonly described qualitatively in most engineering practice and academic research. Methods and indices to quantify particle shape (e.g., Krumbein & Sloss 1963, Wadell 1932, Bowman et al. 2001) may be subjective, inaccurate and tedious in nature. Recently, the QICPIC system, which provides a robust solution to particle shape analysis, has been successfully applied in several investigations to characterize the mechanical properties of soils (e.g., Cavarretta et al. 2010, Yang & Luo 2015, Altuhafi et al. 2016).

It is widely accepted that the initial state of sands (e.g., packing density, effective confining pressure) can affect liquefaction resistance. Recent studies (Yang & Sze 2011a,b, Wei & Yang 2015) have revealed that the state parameter (ψ), proposed by Been & Jefferies (1985) in the framework of critical state soil mechanics, is a rational index to unify the effects of packing density and effective confining pressure on liquefaction resistance of sandy soils, as well as to characterized the effects of initial static shear stress and fines content. In addition, the state parameter can also be applied to characterize various aspects of the mechanical behavior of sandy soils (e.g. Yang 2002, Yang & Li 2004, Jefferies & Been 2006, Murthy et al. 2007, Yang & Liu 2016). The application of the state parameter requires a proper estimation of the critical state parameters. Some recent research has revealed that the critical state parameters can be correlated with particle shape. Yang & Wei (2012) and Wei & Yang (2014) proposed the concept of combined roundness (R_{comb}) to characterize the critical state friction angle of silty sands. Later, the combined concept was extended by Yang & Luo (2015), who further correlated the parameters of the critical state line with the overall regularity of the particles. Noting that the critical state framework is promising in liquefaction analysis, it is of interest to combine these recent findings on the effects of particle shape with the critical-state based framework of liquefaction analysis.

This paper presents experimental results to investigate the liquefaction resistance of clean sands with different particle shapes. The QICPIC system has been used to analyze the particle shapes of the sands. The effects of particle shape on the liquefaction resistance are examined carefully using different shape indices. A unified critical-state based framework of liquefaction analysis is proposed to account for the effects of particle shape.

2 EXPERIMENTAL PROGRAM

2.1 *Testing materials*

The testing materials are manufactured silica sand (MS), Fujian sand (FS) and a mixture of FS and glass bead (GB). Figure 1 presents the SEM images of the tested materials. All the materials were sieved to have the same particle size distribution (Figure 2), making particle shape the only major variable in the study.

The particle characteristics were quantified by Yang & Luo (2015) using QICPIC. The major shape quantities are aspect ratio (AR), sphericity (SPH), and convexity (CVX). The overall regularity (OR) is defined by Equation 1. The parameters for the mixture are calculated following the concept of R_{comb} by Yang & Wei (2012). An example using OR is given in Equation 2.

$$OR = (AR + SPH + CVX)/3 \tag{1}$$

$$OR_{\text{mixture}} = (\text{FS\%}) \cdot OR_{\text{FS}} + (\text{GB\%}) \cdot OR_{\text{GB}} \tag{2}$$

The basic properties of the tested materials are summarized in Table 1. All the tested materials are uniformly graded. MS is the least regular material (lowest OR) and GB is the most

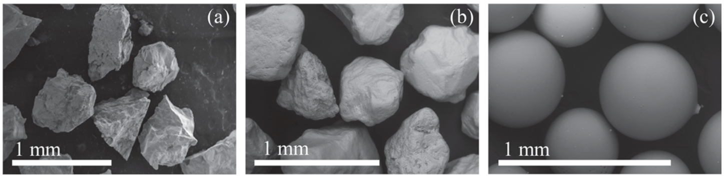

Figure 1. SEM images of the tested materials: (a) manufactured silica sand, (b) Fujian sand, and (c) glass bead.

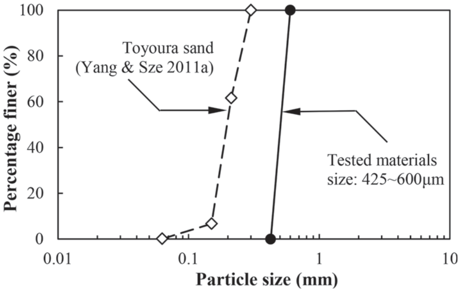

Figure 2. Particle size distribution of the tested materials.

Table 1. Material properties

Material	D_{50}: mm	C_u	AR	SPH	CVX	OR
MS	0.512	1.20	0.695	0.844	0.934	0.825
FS	0.512	1.20	0.745	0.891	0.956	0.864
GB	0.512	1.20	0.974	0.944	0.974	0.964
FS60G40	0.512	1.20	0.837	0.912	0.963	0.904

regular one (highest *OR*). The mixture FS60G40 has an *OR* value in between its two components, i.e. FS and GB.

2.2 *Cyclic triaxial test*

Moist tamping method was adopted to prepare the specimens. Since the cyclic resistance is very sensitive to the degree of saturation (Yang et al. 2004), all specimens were saturated by percolation of CO_2 and de-aired water, followed by applying back pressures (300kPa) to achieve fully saturated condition (B-value greater than 0.98). The specimens were isotropically consolidated to normal effective stress σ'_{nc} = 100kPa, and then loaded under uniform sinusoidal cyclic deviatoric stress cycles with an amplitude of q_{cyc}. The loading magnitude is represented by the cyclic stress ratio ($CSR = q_{cyc}/\sigma'_{nc}$). The void ratio after consolidation (e_c) was determined by measuring the water content after the test.

3 TEST RESULTS

3.1 *Failure patterns*

The failure patterns of tested specimens were in agreement with the findings by Sze & Yang (2014) on clean sand. For loose specimens, the specimens failed in the pattern of flow failure, which is characterized by an abrupt development of large deformations without significant axial strain (< 5%) before failure. The dense specimens failed in the pattern of cyclic mobility

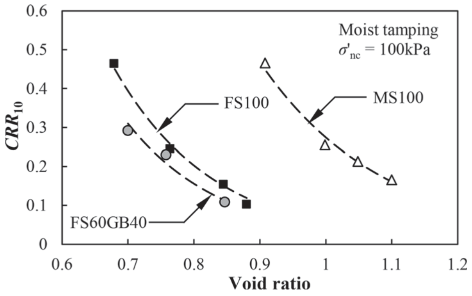

Figure 3. Cyclic resistance of the tested materials at different initial void ratios (for specimen characteristics, see Table 1).

with the attainment of transient zero effective stress. The failure was defined as the onset of flow for loose specimens and as the attainment of 5% double amplitude (D.A.) axial strain for dense ones. The cyclic resistance ratio, *CRR*, was defined as the *CSR* leading to failure in the 10th cycle (i.e. CRR_{10}).

3.2 *Cyclic resistance*

Under the same initial confining pressure (σ_{nc}' = 100kPa), the *CRR-e* data are plotted in Figure 3 for the three materials. All the three materials show that *CRR* decreases with increasing void ratio prior to cyclic loading, but different materials have distinct trend lines. The manufactured silica sand located at the most righthand side, whereas the Fujian sand located between FS60GB40 and MS100. The particle shape is the controlling factor leading to different *CRR-e* relationships because the comparison is made under the same confining pressure and the materials are only different in particle shape. An exponential equation, as follows, can be used to best-fit the data points.

$$CRR_{10} = \alpha \cdot \exp(-\beta \cdot e) \tag{3}$$

where α and β are fitting parameters. The combinations (α, β) for the three materials are MS100 = (57.46, 5.18), FS100 = (41.40, 6.65), FS60GB40 = (38.14, 6.88). Figure 4 plots the fitting parameters α and β against the shape quantities, showing that α decreases with increasing values of the shape quantities, whereas β increases. For each of the two fitting parameters, different shape quantities lead to different correlations, implying that different shape quantities can have different degrees of impact on the cyclic resistance.

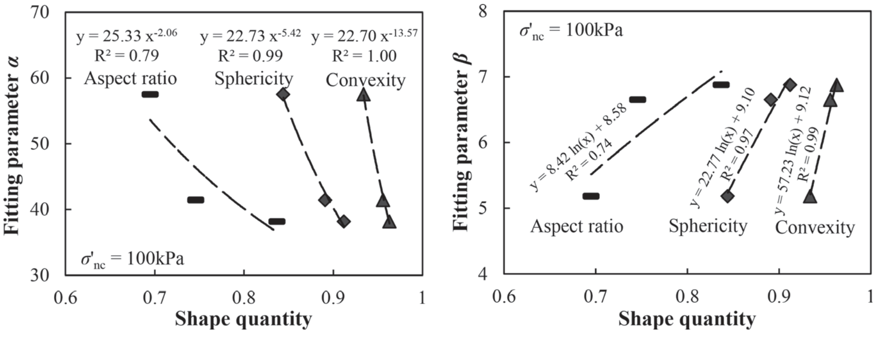

Figure 4. Correlations between the fitting parameters and the shape quantities.

4 CRITICAL-STATE BASED ANALYSIS

The analysis in the previous section indicates that *CRR* is a function of particle shape. However, traditional characterization of shape effects on *CRR* is not easy. This is partly because different shape quantities were found to have certain degrees of impacts on the cyclic resistance, and each of these parameters cannot be isolated. In addition, other factors, such as packing density and confining pressure, can also affect the cyclic resistance.

The critical state theory has been found useful to characterize the liquefaction resistance and other mechanical behaviors of sands, and has been found that it can be applied to unify the effects of initial states and fines content on the cyclic resistance by using the state parameter (Yang & Sze 2011a,b, Wei & Yang 2015). It is of interest to apply the critical state theory to characterize the effects of particle shape on the cyclic resistance.

4.1 *Critical state lines*

The critical state line (CSL) of sand can be formulated using the following equation.

$$e_{CS} = e_{\Gamma} - \lambda_c \left(\frac{p\prime}{P_a} \right)^{0.6} \tag{4}$$

where P_a is a reference pressure equaling to atmospheric pressure; e_Γ and λ_c are parameters of the CSL. For the same materials, Yang and Luo (2015) have found that e_Γ and λ_c decrease with increasing *OR*, and proposed Equation 5 to characterize the experimental data. In other words, the CSL in the *e-p'* plane has a lower position and a more flattened gradient for sands with the more regular shape.

$$e_\Gamma = 2.927 - 2.381 \cdot OR \tag{5a}$$

$$\lambda_c = 0.456 - 0.498 \cdot OR \tag{5b}$$

4.2 *Unifying the effects of particle shape*

In Figure 5, the same framework is applied to the sands with different particle shapes. The trendlines for each of these materials are not exactly the same (Figure 5(a)), but the distance between the three *CRR*-ψ trendlines are much closer than those *CRR*-*e* trend lines shown in Figure 3. The data points are so close to each other, and a unique trend line may be proposed for the three materials (Equation 6). Either a linear or exponential trendline may be suitable for these data, as shown in Figure 5(b).

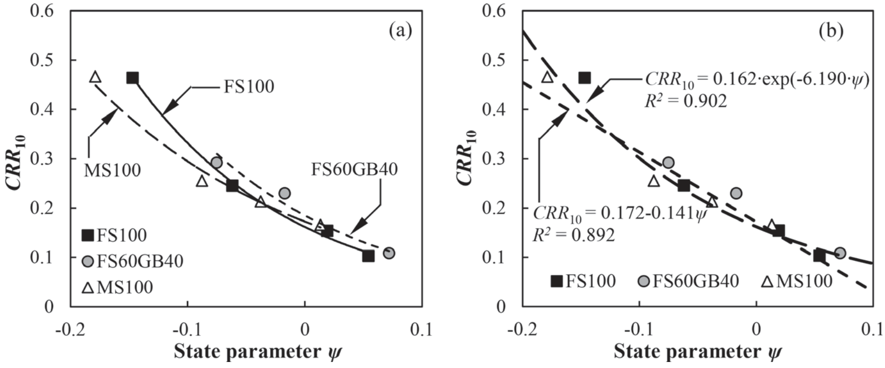

Figure 5. *CRR*-ψ correlations of the three sands with different shapes: (a) material-specific correlations, and (b) unified correlation

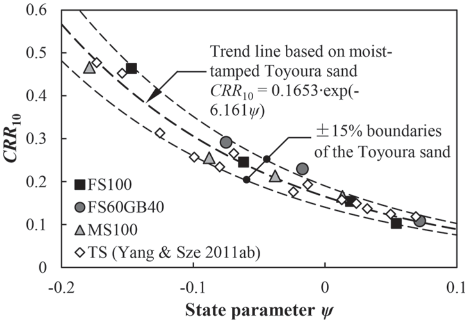

Figure 6. Comparing *CRR*-*ψ* relations with literature data

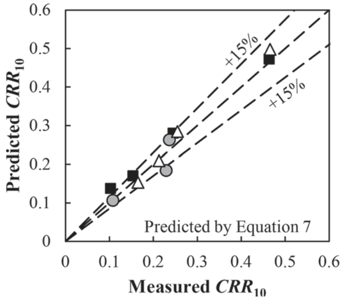

Figure 7. Predicting the cyclic resistance using unified *CRR*-*ψ* correlation

$$CRR_{10} = 0.172 - 0.141 \cdot \psi \tag{6a}$$

$$CRR_{10} = 0.162 \cdot \exp(-6.190 \cdot \psi) \tag{6b}$$

In addition, it is of interest to compare the present data with the data from Yang & Sze (2011a,b) using moist-tamped Toyoura sand (Figure 6). As shown in the figure, the data of the three tested sands fall into the vicinity of the trendline (Equation 7) of the Toyoura sand (±15% of the trendline).

$$CRR_{10} = 0.165 \cdot \exp(-6.161 \cdot \psi) \tag{7}$$

4.3 *Predicting the cyclic resistance*

The unified relationship can be used to predict the cyclic resistance of sands, as long as the initial state parameter is estimated. The initial state parameter for each specimen can be directly obtained using the initial void ratio, confining pressure, and the critical state line in the *e*-*p*' plane. Yang & Luo (2015) reported the critical state line for the specimens tested in this study, and suggested Equation 5 to estimate the critical state line for other sands with the same PSD curve but different particle shape. After the initial state parameter is known, Equation 7 can be applied to predict the cyclic resistance. Figure 7 compares the predicted values with measured values, showing that the prediction agrees well with the measured values since nearly all the data fall into the ±15% of equality.

5 DISCUSSIONS

While the unified *CRR*-*ψ* relationship is promising, it is to be noted that the relationship may depend on the initial fabric formed by the sample preparation method. Jefferies & Been (2016) demonstrated the effects of sample preparation method on the *CSR*-N_1 relationships, showing that the cyclic resistance of the specimens formed by moist methods can be significantly higher than that of the specimens formed by dry methods. A comprehensive study of the effects of sample preparation was conducted by Sze & Yang (2014), who found that the soil fabric formed by dry deposition can lead to unique failure modes different from those of moist-tamped samples in certain situations and the conventional failure criteria based on a certain level of strain or pore-water

pressure do not properly represent the failure mechanism involved and may lead to a substantial overestimation of cyclic resistance in certain situations. Clearly, the fabric should be regarded as a state parameter as important as the conventional ones (i.e. density and confining stress) in describing soil behavior. Future work along the line is worthwhile.

6 CONCLUSIONS

The present study investigated the cyclic behavior and liquefaction resistance of three silica sands with different particle shape. The particles size distributions of the three materials are controlled to eliminate the effects of particle size and particle gradation. Based on the undrained cyclic triaxial tests, the main findings of the present study are summarized as follows.

1. The cyclic resistance of each sand decreases with increasing initial void ratio. When the cyclic resistances of different sands are compared at the same void ratio, CRR increases with decreasing particle regularity, and *vice versa*.
2. But the characterization of the cyclic resistance based on void ratio can be difficult if the shape effects are considered.
3. In the critical state framework, the CRR-ψ data of the three sands located very close to each other. A unique trend can be proposed for these three materials.
4. The data of the present study were compared with Toyoura sand data. Four sets of the data located very close to each other. And the trendline calibrated from the Toyoura sand can be used to unify the CRR-ψ relationships of the four sands. The unified trendline calibrated from Toyoura sand can be used to predict the cyclic resistance of the moist-tamped specimens of the four silica sands.

ACKNOWLEDGEMENT

The study forms part of the research supported by the Research Grants Council of Hong Kong (No. 17250316; 17206418). The financial support provided by the Ministry of Education (MOE) Key Laboratory of Soft Soils and Geoenvironmental Engineering of Zhejiang University (No. 2018P02) is also acknowledged.

REFERENCES

Altuhafi, F.N., Coop, M.R. & Georgiannou, V.N. 2016. Effect of particle shape on the mechanical behavior of natural sands. *Journal of Geotechnical and Geoenvironmental Engineering*, 142(12): 4016071.

Arulmoli, K., Arulanandan, K. & Seed, H.B. 1985. New method for evaluating liquefaction potential. *Journal of Geotechnical Engineering*, 111(1): 95–114.

Been, K. & Jefferies, M. G. 1985. A state parameter for sands. *Géotechnique*, 35(2): 99–112.

Bowman, E.T., Soga, K. & Drummond, W. 2001. Particle shape characterisation using Fourier descriptor analysis. *Géotechnique*, 51(6): 545–554.

Bray, J.D. et al. 2004. Subsurface characterization at ground failure sites in Adapazari Turkey. *Journal of Geotechnical and Geoenvironmental Engineering*, 130(7): 673–685.

Cavarretta, I., Coop, M. & Osullivan, C. 2010. The influence of particle characteristics on the behaviour of coarse-grained soils. *Géotechnique*, 60(6): 413–423.

Cho, G.-C., Dodds, J. & Santamarina, J. C. 2006. Particle shape effects on packing density, stiffness, and strength: natural and crushed sands. *Journal of Geotechnical and Geoenvironmental Engineering*, 132 (5): 591–602.

Hird, C.C. & Hassona, F.A.K. 1990. Some factors affecting the liquefaction and flow of saturated sands in laboratory tests. *Engineering Geology*, 28(1–2): 149–170.

Holubec, I. & D'appolonia, E. 1973. Effect of particle shape on the engineering properties of granular soils. In E.T. Selig & R.S. Ladd (eds), *Evaluation of Relative Density and its Role in Geotechnical Projects Involving Cohesionless Soils*. Philadelphia: ASTM International.

Jefferies, M.G. & Been, K. 2006 & 2016. *Soil Liquefaction: A Critical State Approach* (1st & 2nd edns). Boca Raton: CRC Press.

Kramer, S.L. 1996. *Geotechnical Earthquake Engineering*. New Jersey: Printice Hall.

Krumbein, W.C. & Sloss, L.L. 1963. *Stratigraphy and Sedimentation* (2nd edn.). San Francisco: W.H. Freeman and Company.

Murthy, T.G. et al. 2007. Undrained monotonic response of clean and silty sands. *Géotechnique*, 57(3): 273–288.

Rousé, P.C., Fannin, R.J. & Shuttle, D. A. 2008. Influence of roundness on the void ratio and strength of uniform sand. *Géotechnique*, 58(3): 227–231.

Sze, H. Y. & Yang, J. 2014. Failure modes of sand in undrained cyclic loading: impact of sample preparation. *Journal of Geotechnical and Geoenvironmental Engineering* 140(1): 152–169.

Wadell, H. 1932. Volume, shape, and roundness of rock particles. *The Journal of Geology*, 40(5): 443–451.

Wei, L.M. & Yang, J. 2014. On the role of grain shape in static liquefaction of sand–fines mixtures. *Géotechnique*, 64(9): 740–745.

Wei, X. & Yang, J. 2015. The effects of initial static shear stress on liquefaction resistance of silty sand. In *Proceedings of 6th International Conference on Earthquake Geotechnical Engineering*. 1–4 November 2015. Christchurch, New Zealand.

Yang, J. 2002. Non-uniqueness of flow liquefaction line for loose sand. *Géotechnique*, 52(10): 757–760.

Yang, J. & Li, X.S. 2004. State-dependent strength of sands from the perspective of unified modeling. *Journal of Geotechnical and Geoenvironmental Engineering*, 130(2): 186–198.

Yang, J. & Liu, X. 2016. Shear wave velocity and stiffness of sand: the role of non-plastic fines. *Géotechnique*, 66(6): 500–514.

Yang, J. & Luo, X.D. 2015. Exploring the relationship between critical state and particle shape for granular materials. *Journal of the Mechanics and Physics of Solids*, 84, 196–213.

Yang, J., Savidis, S. & Roemer, M. 2004. Evaluating liquefaction strength of partially saturated sand. *Journal of Geotechnical and Geoenvironmental Engineering*, 130(9): 975–979.

Yang, J. & Sze, H.Y. 2011a. Cyclic behaviour and resistance of saturated sand under non-symmetrical loading conditions. *Géotechnique*, 61(1): 59–73.

Yang, J. & Sze, H.Y. 2011b. Cyclic strength of sand under sustained shear stress. *Journal of Geotechnical and Geoenvironmental Engineering*, 137(12): 1275–1285.

Yang, J. & Wei, L.M. 2012. Collapse of loose sand with the addition of fines: the role of particle shape. *Géotechnique*, 62(12): 1111–1125.

Youd, T.L. 1973. Factors controlling maximum and minimum densities of sands. In E.T. Selig & R.S. Ladd (eds), *Evaluation of Relative Density and its Role in Geotechnical Projects Involving Cohesionless Soils*. Philadelphia: ASTM International.